

# Low-mass neutron stars: universal relations, the nuclear symmetry energy and gravitational radiation

Hector O. Silva<sup>1\*</sup>, Hajime Sotani<sup>2†</sup>, Emanuele Berti<sup>1,3‡</sup>

<sup>1</sup>*Department of Physics and Astronomy, The University of Mississippi, University, Mississippi 38677, USA*

<sup>2</sup>*Division of Theoretical Astronomy, National Astronomical Observatory of Japan, 2-21-1 Osawa, Mitaka, Tokyo 181-8588, Japan*

<sup>3</sup>*CENTRA, Departamento de Física, Instituto Superior Técnico, Universidade de Lisboa, Avenida Rovisco Pais 1, 1049 Lisboa, Portugal*

Accepted XXX. Received YYY; in original form ZZZ

## ABSTRACT

The lowest neutron star masses currently measured are in the range  $1.0 - 1.1 M_{\odot}$ , but these measurements have either large uncertainties or refer to isolated neutron stars. The recent claim of a precisely measured mass  $M/M_{\odot} = 1.174 \pm 0.004$  (Martinez et al. 2015) in a double neutron star system suggests that low-mass neutron stars may be an interesting target for gravitational-wave detectors. Furthermore, Sotani et al. (2014) recently found empirical formulas relating the mass and surface redshift of nonrotating neutron stars to the star’s central density and to the parameter  $\eta \equiv (K_0 L^2)^{1/3}$ , where  $K_0$  is the incompressibility of symmetric nuclear matter and  $L$  is the slope of the symmetry energy at saturation density. Motivated by these considerations, we extend the work by Sotani et al. (2014) to slowly rotating and tidally deformed neutron stars. We compute the moment of inertia, quadrupole moment, quadrupole ellipticity, tidal and rotational Love number and apsidal constant of slowly rotating neutron stars by integrating the Hartle-Thorne equations at second order in rotation, and we fit all of these quantities as functions of  $\eta$  and of the central density. These fits may be used to constrain  $\eta$ , either via observations of binary pulsars in the electromagnetic spectrum, or via near-future observations of inspiralling compact binaries in the gravitational-wave spectrum.

**Key words:** stars: neutron – stars: rotation – equation of state

## 1 INTRODUCTION

The equilibrium of spherically symmetric, nonrotating neutron stars (NSs) in general relativity is governed by the Tolman-Oppenheimer-Volkoff (TOV) equations, that follow from Einstein’s equations with a perfect-fluid stress energy tensor (see e.g. Stergioulas 2003; Shapiro & Teukolsky 1983; Friedman & Stergioulas 2013). When supplemented with an equation of state (EOS) relating the density and pressure of the perfect fluid, the TOV equations form a closed system of ordinary differential equations, whose solutions are obtained (in general) by numerical integration. The solutions form a single-parameter family, where the parameter can be chosen to be the central total energy density  $\rho_c$ . Despite recent progress, the EOS is still largely unknown at the energy densities  $\rho > \rho_0$  (where  $\rho_0/c^2 \equiv 2.68 \times 10^{14}$  g/cm<sup>3</sup> is the nuclear saturation density) characterizing the NS core. Uncertainties in the EOS translate into uncertain-

ties in the NS mass-radius relation: for a typical NS mass  $M \sim 1.4 M_{\odot}$ , EOSs compatible with our current knowledge of nuclear physics predict radii  $R$  ranging between 6 and 16 km (Steiner et al. 2013).

Unlike black holes, which are vacuum solutions of Einstein’s equations, NS structure depends on the coupling of gravity with matter. Therefore NSs can probe (and possibly rule out) theories of gravity that are close to general relativity in vacuum, but differ in the description of the coupling between matter and gravity in the strong-field regime (Berti et al. 2015). In fact, given the strength of their gravitational field, the high density of matter at their cores and the existence of pulsars with fast spin and large magnetic fields, NSs are ideal laboratories to study all fundamental interactions (Lattimer & Prakash 2004, 2007, 2015; Psaltis 2008). However, tests of strong gravity with NSs are made more difficult by two fundamental degeneracies: (i) uncertainties in the EOS can mimic the modifications to the bulk properties of NSs that may be induced by hypothetical strong-field modifications of general relativity; (ii) different theories of gravity can give rise to similar modifications in the bulk properties of NSs (Glampedakis et al. 2015).

\* E-mail: hosilva@phy.olemiss.edu

† E-mail: sotani@yukawa.kyoto-u.ac.jp

‡ E-mail: eberti@olemiss.edu

These issues are partially alleviated by recently discovered “universal” (EOS-independent) relations showing that NSs are, in fact, relatively simple objects. Let  $M$  be the mass of a nonrotating star,  $\chi = J/M^2$  the dimensionless spin (here and below we use geometrical units,  $G = c = 1$ ),  $I$  the moment of inertia,  $Q$  the quadrupole moment and  $\lambda^{(\text{tid})}$  the tidal Love number, a measure of stellar deformability. Working in the slow-rotation approximation, Yagi & Yunes (2013b,a) discovered that universal (EOS-independent) “ $I$ -Love- $Q$ ” relations connect the three normalized quantities  $\bar{I} = I/M^3$ ,  $\bar{\lambda}^{(\text{tid})} = \lambda^{(\text{tid})}/M^5$  and  $\bar{Q} = -Q^{(\text{rot})}/(M^3\chi^2)$ . Subsequent work relaxed the slow-rotation approximation, showing that the universality still holds (Doneva et al. 2013; Pappas & Apostolatos 2014; Chakrabarti et al. 2014; Yagi et al. 2014a).

Most investigations of relativistic stellar structure focus on NSs with the “canonical”  $1.4M_\odot$  mass or higher. From a nuclear physics standpoint, recent measurements of masses  $M \gtrsim 2M_\odot$  have ruled out EOS models that are unable to support such high masses (Demorest et al. 2010; Antoniadis et al. 2013)<sup>1</sup>. Large-mass NSs are more compact, and therefore more interesting for tests of strong gravity. From an astrophysical point of view, the large-mass regime is also interesting to improve our understanding of core-collapse physics. Observations of NS binaries (particularly via radio pulsars) and black hole X-ray binaries indicate that there may be a mass gap between the two populations: the highest measured NS masses just exceed  $2M_\odot$  (Lattimer 2012), while black hole masses may only start at  $\sim 4\text{--}5.5M_\odot$  (Ozel et al. 2010; Farr et al. 2011), depending on the assumed shape of the distribution (but see Kreidberg et al. 2012, who point out that selection biases could yield lower black hole masses). Gravitational-wave observations of merging compact binaries will offer a unique opportunity to probe the existence of this “mass gap” (Dominik et al. 2015; Mandel et al. 2015; Littenberg et al. 2015; Stevenson et al. 2015; Belczynski et al. 2015; Chatziioannou et al. 2015a).

Our focus here is instead on low-mass NSs. There are observational and theoretical reasons why this regime is interesting. The lowest well-constrained NS masses currently measured are in the range  $1.0\text{--}1.1 M_\odot$  (Lattimer 2012). Recently Martinez et al. (2015) claimed a precise measurement of  $M/M_\odot = 1.174 \pm 0.004$  in a double NS system with large mass asymmetry. While the minimum mass of a star constructed from a cold dense matter EOS is quite small ( $< 0.1M_\odot$ ), the minimum mass of a hot protoneutron star is considerably larger, in the range  $0.89\text{--}1.13M_\odot$  for the models considered by Strobel et al. (1999). This minimum mass provides a practical lower bound on NS masses formed from supernovae, unless lower-mass stars form by fragmentation (see e.g. the speculative scenario of Popov et al. 2007). Estimates based on the baryonic mass of the iron core of the supernova progenitor give a minimum mass of  $\sim 1.15\text{--}1.2M_\odot$ , as discussed in Sec. 3.3 of Lattimer (2012). Tauris et al. (2015) estimate that the minimum mass of a NS

formed in an ultra-stripped supernova is  $1.1M_\odot$ . Note that uncertainties in supernova physics affect all of these bounds, and (if confirmed) the recent observations of Martinez et al. (2015) may challenge the iron core bound. To summarize: it is commonly believed that the minimum mass of NSs in the universe should be around the minimum observed mass ( $\sim 1M_\odot$ ) and that NS masses  $\lesssim 1.2M_\odot$  would challenge the paradigm of NS formation by gravitational collapse, but these conclusions are uncertain due to our limited understanding of supernova physics. Therefore the discovery of low-mass NSs may give us important clues on their formation mechanism: for example, observations of NSs with mass  $M \lesssim 1M_\odot$  could validate the astrophysical viability of the proto-NS fragmentation scenario proposed by Popov et al. (2007).

Another key motivation for this work is that the low-mass regime is sensitive to – and carries information on – the isospin dependence of nuclear forces, and in particular on the nuclear symmetry energy (Steiner et al. 2005; Tsang et al. 2012; Li & Han 2013; Lattimer & Steiner 2014; Li et al. 2014; Newton et al. 2014). Sotani et al. (2014) recently computed the structure of low-mass nonrotating NSs for a wide range of EOSs. They found that their mass  $M$  and surface redshift  $z$  can be fitted by simple functions of the central density  $\rho_c$  and of the dimensionful parameter

$$\eta \equiv (K_0 L^2)^{1/3}, \quad (1)$$

where  $K_0$  is the incompressibility of symmetric nuclear matter and  $L$  is the slope of the symmetry energy at saturation density (note that  $K_0$ ,  $L$  and  $\eta$  all have units of energy). Therefore, at least in principle, measurements of  $M$  and  $z$  could be used to constrain  $\eta$ ; in fact, the NS radius is highly correlated with the NS matter pressure at densities close to nuclear saturation density. A practical complication is that the determination of  $z$  and of the stellar radius, e.g. via photospheric radius expansion bursts and thermal emissions from quiescent low-mass X-ray binaries, is model-dependent and affected by systematic errors. Therefore, at present, no individual observation can determine NS radii to better than  $\sim 20\%$  accuracy. This translates into nearly a 100% error in the determination of  $L$ , since  $L \sim R^4$  (Lattimer & Steiner 2014).

A possible way to circumvent this problem is to rely on the fact that all NSs in nature are spinning. Considering rotating NSs is of interest because near-future experiments in the electromagnetic spectrum – such as NICER (Gendreau et al. 2012), LOFT (Feroci et al. 2012), Astro-H (Takahashi et al. 2012) and SKA (Watts et al. 2015) – or in the gravitational-wave spectrum – such as Advanced LIGO (Aasi et al. 2015), Advanced Virgo (Acernese et al. 2015), KAGRA (Somiya 2012) and the Einstein Telescope (Sathyaprakash et al. 2012) – could measure or constrain the additional multipoles that determine the structure of rotating NSs or other properties (such as the “Love numbers”) that are related to their deformability. Spin-orbit coupling in binary pulsars may allow us to measure the moment of inertia (Damour & Schaefer 1988; Lattimer & Schutz 2005; Bejger et al. 2005; Kramer & Wex 2009) and gravitational-wave observations may be used to infer the tidal Love numbers, as well as additional information on the EOS (Mora & Will 2004; Berti et al. 2008; Flanagan & Hinderer

<sup>1</sup> Here we will consider some EOS models that do not respect this constraint. This is because we are primarily interested in densities  $\rho \sim \rho_0$ , and (conservatively) we assume no correlation between the EOS near the saturation density and the EOS at higher densities (cf. Steiner et al. 2015).

2008; Read et al. 2009; Hinderer et al. 2010; Vines et al. 2011; Damour et al. 2012; Del Pozzo et al. 2013; Read et al. 2013; Favata 2014; Yagi & Yunes 2014; Lackey et al. 2014; Chatziioannou et al. 2015b; Yagi & Yunes 2015; Dietrich et al. 2015). Quite remarkably, measurements of the moment of inertia within an accuracy  $\sim 10\%$  *alone* can yield tight constraints on the pressure over a range of densities (Steiner et al. 2015). The correlation between the moment of inertia and the tidal deformability (the “*I*-Love” relation) is very tight for massive NSs (Yagi & Yunes 2013b,a), but not so much in the low-mass regime: see e.g. Fig. 3 below.

One of the main results of the present work is that all of the properties of rotating and tidally deformed stars can be expressed as simple functions of  $\rho_c$  and  $\eta$ . Therefore measurements of any two bulk properties of a low-mass NS – for example, the mass  $M$  and the moment of inertia  $I$  – can be used to constrain  $\eta$ : one measurement is necessary to pin down  $\rho_c$ , and the second can determine  $\eta$ .

The plan of the paper is as follows. In Section 2 we discuss the EOS models used in this paper and the properties of nuclear matter that are relevant in the low-mass regime. In Section 3 we present our numerical results for the bulk properties of nonrotating and slowly rotating NSs, and we fit the properties of slowly rotating NSs by nearly universal functions of the central density  $\rho_c$  and of the parameter  $\eta$ . In the concluding Section 4 we discuss possible observational applications and future extensions of our work.

## 2 LOW-MASS NEUTRON STAR PROPERTIES AND THE NUCLEAR SYMMETRY ENERGY

In this section we introduce some notation for the properties of uniform nuclear matter near saturation density, and we describe the EOS models used in our numerical work.

### 2.1 Properties of uniform nuclear matter

The energy of uniform nuclear matter at zero temperature can be expanded around the saturation point of symmetric nuclear matter (i.e., matter composed of an equal number of neutrons and protons). If  $n_b$  is the nucleon number density and  $\alpha \equiv (n_n - n_p)/n_b$ , where  $n_n$  ( $n_p$ ) is the neutron (proton) number density, the bulk energy per nucleon  $w$  of uniform nuclear matter can be written as

$$w = w_0 + \frac{K_0}{18n_0^2}(n_b - n_0)^2 + \left[ S_0 + \frac{L}{3n_0}(n_b - n_0) \right] \alpha^2, \quad (2)$$

where  $w_0$ ,  $n_0$  and  $K_0$  are the saturation energy, the saturation density and the incompressibility of symmetric nuclear matter, while  $S_0$  and  $L$  are associated with the symmetry energy coefficient  $S(n_b)$ :

$$S_0 = S(n_0), \quad L = 3n_0 \left( \frac{dS}{dn_b} \right) \Big|_{n_b=n_0}. \quad (3)$$

The parameters  $w_0$ ,  $n_0$  and  $S_0$  can be relatively easily determined from empirical data for the masses and radii of stable nuclei. The parameters  $K_0$  and  $L$ , which determine the stiffness of neutron-rich nuclear matter, are more difficult to fix, and they affect the structure of low-mass NSs.

Different EOS models are based on different theoretical and computational approaches in nuclear physics. In

**Table 1.** Parameters of the EOSs used in this work. EOSs which result in NSs with a maximum mass larger than  $2M_\odot$  are indicated by an asterisk.

EOS	$K_0$ (MeV)	$L$ (MeV)	$\eta$ (MeV)
OI 180/220	180	52.2	78.9
OI 230/350	230	42.6	74.7
OI 230/220	230	73.4	107
OI 280/350	280	54.9	94.5
OI 280/220*	280	97.5	139
OI 360/350*	360	76.4	128
OI 360/220*	360	146	197
Shen*	281	114	154
Miyatsu	274	77.1	118
FPS	261	34.9	68.2
SLy4*	230	45.9	78.5
BSk19	237	31.9	62.3
BSk20*	241	37.9	69.6
BSk21*	246	46.6	81.1

order to derive empirical formulas expressing the properties of low-mass NSs that do not rely on specific EOSs, following Sotani et al. (2014) we adopt several tabulated EOS models that can be separated into three categories:

(1) The phenomenological EOS model constructed by Oyamatsu and Iida (Oyamatsu & Iida 2003). The bulk energy  $w(n_b, \alpha)$  is constructed to reproduce Eq. (2) in the limit where  $n_b \rightarrow n_0$  and  $\alpha \rightarrow 0$ , and the optimal values of  $w_0$ ,  $n_0$ , and  $S_0$  are determined by requiring that the density profile of stable nuclei (determined within the extended Thomas-Fermi theory for given values of  $L$  and  $K_0$ ) reproduce experimental nuclear data. The EOSs in this category will be labeled as OI  $K/Y$ , where  $K = K_0$  and  $Y = -K_0 S_0 / (3n_0 L)$ . At variance with Sotani et al. (2014) we will omit the OI 180/350 EOS, because the associated values of  $K_0$  and  $L$  are ruled out by current nuclear physics constraints (cf. Sec. 2.2).

(2) Two EOS models based on the relativistic framework. One of these models (Shen) is constructed within relativistic mean field theory together with the TM1 nuclear interaction (Shen et al. 1998); the second (Miyatsu) is based on the relativistic Hartree-Fock theory with the chiral quark-meson coupling model (Miyatsu et al. 2013). The spherical nuclei in the crust region are determined using the Thomas-Fermi theory.

(3) Five EOS models based on the Skyrme-type effective interactions: FPS, SLy4, BSk19, BSk20, and BSk21 (Lorenz et al. 1993; Douchin & Haensel 2001; Goriely et al. 2010; Pearson et al. 2011, 2012; Potekhin et al. 2013).

All of these models are *unified* EOSs, i.e., both the crust and core regions can be described with the same EOS with specific values of  $K_0$  and  $L$ . From the EOS tables we can compute  $K_0$ ,  $L$  and the auxiliary dimensionful parameter  $\eta$  introduced in Eq. (1) above, with the results listed in Table 1. The mass-radius relations predicted by these EOS models for nonrotating low-mass NSs are shown in Fig. 1.

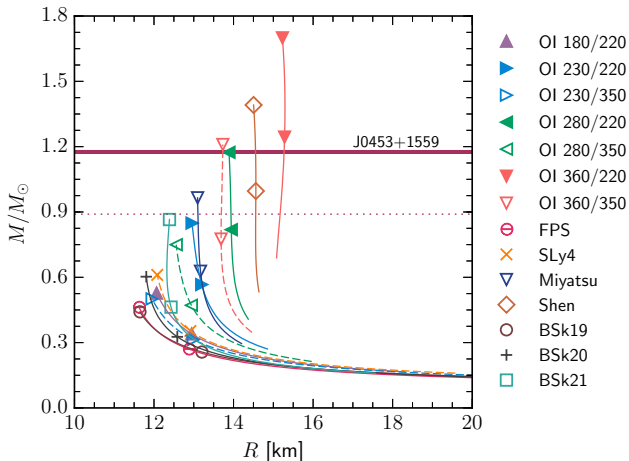


**Figure 1.** Mass-radius relations for the EOSs adopted in this paper, and discussed in Sec. 2. Each line covers the range  $u_c = \rho_c/\rho_0 \in [1, 2]$  for a specific EOS, as indicated in the legend. The solid horizontal band corresponds to the lowest high-precision NS mass measurement of  $M/M_\odot = 1.174 \pm 0.004$  (from [Martinez et al. 2015](#)). The dotted horizontal line indicates a conservative lower bound on the mass of  $M/M_\odot = 0.89$  (see e.g. [Strobel et al. 1999](#)). Symbols on each line correspond to  $u_c = 1.5$  and  $u_c = 2.0$ , respectively.

## 2.2 Experimental constraints

An extensive discussion of theoretical and experimental constraints on the properties of uniform nuclear matter can be found in [Li & Han \(2013\)](#), [Lattimer & Steiner \(2014\)](#) and [Newton et al. \(2014\)](#). Generally accepted values of  $K_0$  are in the range  $K_0 = 230 \pm 40$  MeV ([Khan & Margueron 2013](#)). The current consensus in the nuclear physics community is that values of  $L$  in the range  $L = 60 \pm 20$  MeV are plausible<sup>2</sup> but higher values are not excluded ([Newton et al. 2014](#)).

There are proposals to constrain nuclear saturation parameters, and in particular the value of  $L$ , via astronomical observations. This approach is completely different from constraints based on nuclear physics experiments. Under the assumption that the observed frequencies of quasiperiodic oscillations (QPOs) are related to crustal torsional oscillations, [Sotani et al. \(2013\)](#) found the constraint  $101 < L < 131$  MeV when all the observed frequencies are interpreted as torsional oscillations, or  $58 < L < 85$  MeV when the second lowest frequency is assumed to have a different origin. The inclusion of electron screening effects can modify the constraint on  $L$  to the range  $97 < L < 127$  MeV, instead of  $101 < L < 131$  MeV ([Sotani et al. 2016](#)). Furthermore, in some cases having information on the mass and radius of low-mass NSs may allow us to constrain EOS parameters. For example, the observation of the X-ray burster 4U 1724-307 by [Suleimanov et al. \(2011\)](#) allowed [Sotani et al. \(2015\)](#) to set the constraint  $\eta \gtrsim 130$  MeV. These astrophysical constraints seem incompatible with constraints on  $L$  obtained from the terrestrial nuclear exper-

<sup>2</sup> [Lattimer & Steiner \(2014\)](#) suggest a tighter plausible range of  $44 \text{ MeV} < L < 66 \text{ MeV}$  (see the discussion of their Figure 1), but we will follow [Newton et al. \(2014\)](#) in an attempt to be more conservative.

iments quoted above ([Li & Han 2013](#); [Lattimer & Steiner 2014](#); [Newton et al. 2014](#)). One possible reason for this discrepancy may be that the constraints from nuclear experiments were obtained from almost stable nuclei, whose neutron excess  $\alpha$  in Eq. (2) is very small, while NS matter deviates significantly from symmetric nuclear matter. Indeed, some nuclear experiments with unstable nuclei suggest the possibility that  $L$  may have larger values ([Tsang et al. 2009](#); [Yasuda et al. 2013](#)).

If we adopt as fiducial values  $40 \text{ MeV} < L < 80 \text{ MeV}$  – recalling that higher values cannot be excluded ([Newton et al. 2014](#)) – and  $K_0 = 230 \pm 40$  MeV ([Khan & Margueron 2013](#)), respectively, we can conclude that a plausible range for  $\eta$  is  $67 < \eta < 120$ , and that higher values of  $\eta$  may be possible. This should be kept in mind in Section 3 below, where we discuss how the bulk properties of NSs depend on  $\eta$ .

## 3 NEUTRON STAR STRUCTURE

### 3.1 Nonrotating neutron stars

For nonrotating NSs, the effect of the nuclear symmetry parameters introduced above on the mass-radius relation  $M(R)$  was investigated by [Sotani et al. \(2014\)](#). The main finding of their work was that the NS mass  $M$  and the surface gravitational redshift  $z$ , defined as

$$z = \left(1 - \frac{2M}{R}\right)^{-1/2} - 1, \quad (4)$$

can be expressed as smooth functions of  $\eta$  of the form

$$y = c_0 + c_1 \left(\frac{\eta}{100 \text{ MeV}}\right), \quad (5)$$

where  $y$  collectively denotes either  $M$  or  $z$ . We also note that these relations can be combined to write the radius  $R$  as a function of  $\eta$ .

The coefficients  $c_i$  depend on the ratio  $u_c \equiv \rho_c/\rho_0$  which specifies the central density of the stellar model. Following [Sotani et al. \(2014\)](#), we will fit these coefficient using a quadratic polynomial in  $u_c$ :

$$c_i = c_{i,0} + c_{i,1} u_c + c_{i,2} u_c^2. \quad (6)$$

Therefore each of our empirical formulas will depend on six constant parameters  $c_{i,j}$ .

In Fig. 2 we confirm the main results of [Sotani et al. \(2014\)](#). The left (right) panel shows that, quite independently of the chosen EOS, the mass  $M$  (the redshift  $z$ , respectively) is indeed well fitted by a linear function of  $\eta$  for any fixed value of the central density  $u_c$ : the plots show this explicitly in the three cases  $u_c = 1$ ,  $u_c = 1.5$  and  $u_c = 2$ . The bottom insets show that the fractional differences  $\delta y \equiv |y_{\text{data}} - y_{\text{fit}}|/y_{\text{data}}$  for  $M$  and  $z$  are typically below  $\sim 10\%$  (with the exception of EOS BSk21) whenever  $\eta \gtrsim 67$  MeV.

The values of the fitting constants are listed in the top two rows of Table 2. To quantify the accuracy of these fits, Table 2 also lists the rms relative error ([Lau et al. 2010](#))

$$\sigma \equiv \sqrt{\frac{1}{N} \sum_{i=1}^N \left(1 - \frac{y_i^{\text{fit}}}{y_i^{\text{data}}}\right)^2}, \quad (7)$$

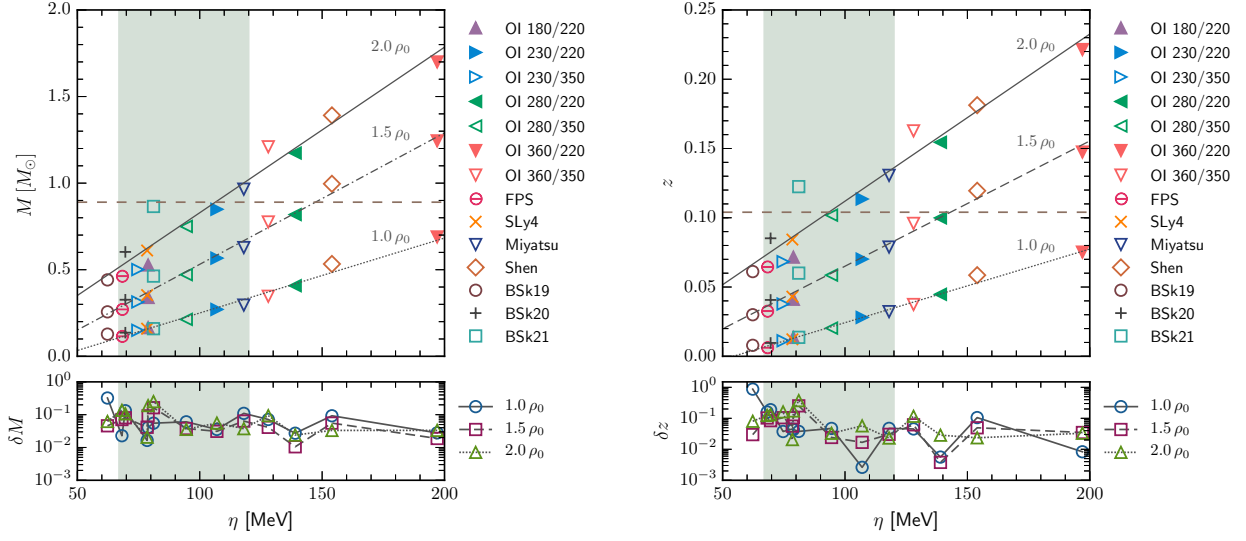


**Figure 2.** *Left:* Dependence of the NS mass  $M$  for a nonrotating star on the parameter  $\eta$  introduced in Eq. (1) at three given values of the central density:  $u_c \equiv \rho_c/\rho_0 = 1.0, 1.5, 2.0$ . *Right:* same, but for the surface gravitational redshift  $z$  defined in Eq. (4). In both cases, the solid lines represent the fit given in Eq. (5) using the fitting parameters listed in Table 2. The lower panels show the relative error of the fit with respect to the numerical data,  $|y_{\text{data}} - y_{\text{fit}}|/y_{\text{data}}$ , as a function of  $\eta$ . The shaded area corresponds to the most plausible range of values for  $\eta$ , namely  $67 < \eta < 120$  (see Sec. 2.2). This plot reproduces and extends Fig. 2 of Sotani et al. (2014). Horizontal dashed lines correspond to a NS with  $M/M_\odot = 0.89$  (the value of  $z$  was computed using the Shen EOS).

**Table 2.** Numerical values of the constant in the fitting expressions and of the rms percentage error  $\sigma$  (last column), computed with / without EOS BSk21.

Using Eqs. (5) and (6) – Quantities at order $\mathcal{O}(\epsilon^0)$ in rotation							
Quantity	$c_{0,0}$	$c_{0,1}$	$c_{0,2}$	$c_{1,0}$	$c_{1,1}$	$c_{1,2}$	$\sigma$
$M$	0.34626	-0.82183	0.29265	-0.60780	1.2996	-0.25890	0.086 / 0.076
$z = (1 - 2M/R)^{-1/2} - 1$	0.0040470	-0.059527	0.026591	-0.042719	0.10673	-0.014208	0.100 / 0.089
Using Eqs. (9) and (6) – Quantities at order $\mathcal{O}(\epsilon^1)$ and $\mathcal{O}(\epsilon^2)$ in rotation							
Quantity	$c_{0,0}$	$c_{0,1}$	$c_{0,2}$	$c_{1,0}$	$c_{1,1}$	$c_{1,2}$	$\sigma$
$\bar{I} = I/M^3$	4.1429	-2.2458	0.46120	-0.23654	-0.26292	0.083322	0.122 / 0.083
$\bar{Q} = -Q^{(\text{rot})} / (M^3 \chi^2)$	2.9160	-1.3835	0.24677	-0.25594	-0.093784	0.015956	0.120 / 0.114
$\bar{\lambda}^{(\text{rot})} = \lambda^{(\text{rot})} / M^5$	11.203	-5.8769	1.1697	-0.24302	-0.21457	0.055320	0.424 / 0.237
$k_2^{(\text{rot})} = (3/2)\lambda^{(\text{rot})} / R^5$	-3.9878	3.3914	-0.91026	-3.4378	2.6267	-0.53179	0.273 / 0.272
$e_Q^* = -Q^{(\text{rot})} / I$	-2.1203	1.8784	-0.52335	-4.0307	3.0883	-0.55984	0.129 / 0.126
Using Eqs. (9) and (6) – Tidally deformed star							
Quantity	$c_{0,0}$	$c_{0,1}$	$c_{0,2}$	$c_{1,0}$	$c_{1,1}$	$c_{1,2}$	$\sigma$
$\bar{\lambda}^{(\text{tid})} = \lambda^{(\text{tid})} / M^5$	11.238	-5.9413	1.1450	-0.21434	-0.25432	0.052281	0.462 / 0.263

where the sum runs over all stellar models  $i = 1, \dots, N$ . Two EOS models, namely BSk20 and BSk21 (and particularly the latter), deviate more from our best-fit function as  $\rho_c$  increases. As pointed out by Sotani et al. (2014), these deviations are of the order of the uncertainties on the mass  $M$  due to three-neutron interactions obtained from the quantum Monte Carlo evaluations (Gandolfi et al. 2012). Therefore in Table 2 we list the values of  $\sigma$  obtained either including or omitting EOS BSk21, the EOS for which the errors are larger.

### 3.2 Slowly rotating and tidally deformed neutron stars

In general, rotating stellar models in general relativity must be constructed numerically by solving a complicated system of partial differential equations. These numerical calculations (reviewed in Stergioulas 2003; Friedman & Stergioulas 2013) suggest that uniformly rotating NSs with physically motivated EOSs have dimensionless angular momentum  $\chi \lesssim 0.7$  (Cook et al. 1994; Berti & Stergioulas 2004; Lo & Lin 2011), but the spin magnitudes of NSs

in binary systems observable by Advanced LIGO are likely to be much smaller than this theoretical upper bound (Mandel & O’Shaughnessy 2010; Brown et al. 2012). The spin period of isolated NSs at birth should be in the range 10–140 ms (or  $\chi \lesssim 0.04$ , Lorimer 2001). Accretion from a binary companion can spin up NSs, but it is unlikely to produce periods less than 1 ms (i.e.  $\chi \lesssim 0.4$ , Chakrabarty 2008). The fastest spinning observed pulsar, PSR J1748–2446ad, has a period of 1.4 ms ( $\chi \sim 0.3$ , Hessels et al. 2006); the fastest known pulsar in a NS–NS system, J0737–3039A, has a period of 22.70 ms ( $\chi \sim 0.02$ , Burgay et al. 2003).

The slow-rotation approximation is basically an expansion in terms of the small parameter  $\epsilon \equiv \Omega/\Omega^* \ll 1$ , where  $\Omega$  is the stellar angular velocity and  $\Omega^* \equiv \sqrt{M/R^3}$  is a characteristic rotation frequency, comparable in order of magnitude to the mass-shedding frequency of the star. Even the fastest known millisecond pulsar (Hessels et al. 2006) spins well below the estimated  $\epsilon \approx 0.5$  for which the Hartle–Thorne approximative scheme agrees very well with full numerical calculations (Berti et al. 2005). Therefore the slow-rotation approximation is more than adequate to extend the work on low-mass NSs by Sotani et al. (2014).

The formalism to construct slowly rotating NS models was developed in the seminal works by Hartle (1967) and Hartle & Thorne (1968). Subsequent work extended the formalism up to fourth order in  $\epsilon$ , showing that the equilibrium properties of slowly rotating solutions compare favorably with numerical codes for arbitrary rotation rates even for PSR J1748–2446ad (Berti et al. 2005; Benhar et al. 2005; Yagi et al. 2014a).

We use the stellar structure equations as presented by Sumiyoshi et al. (1999), correcting the misprints listed by Berti et al. (2005). Our numerical results were validated by comparison against the tables by Berti et al. (2005). For the dimensionless bulk properties we follow the definitions of Yagi & Yunes (2013b). The explicit form of the structure equations, their derivation and details of the integration procedure can be found in these references.

At order  $\mathcal{O}(\epsilon^0)$  in the perturbative expansion, a static nonrotating star is characterized by its gravitational mass  $M$  and radius  $R$ . Sometimes it is useful to replace the radius by the surface redshift  $z$  defined in Eq. (4).

At first order in rotation, i.e.  $\mathcal{O}(\epsilon^1)$ , the star is also characterized by its moment of inertia  $I$ . Given  $I$ , we can define a dimensionless moment of inertia  $\bar{I} \equiv I/M^3$  as well as a spin parameter  $\chi \equiv I\Omega/M^2$  (Yagi & Yunes 2013b).

At second order in rotation, i.e.  $\mathcal{O}(\epsilon^2)$ , the star deviates from its spherical shape and acquires a rotational quadrupole moment  $Q^{(\text{rot})^*}$ . For convenience, we define the dimensionless rotation-induced quadrupole moment  $\bar{Q} \equiv -Q^{(\text{rot})^*}/(M^3\chi^2)$ . The  $\ell = 2$  rotational Love number  $\lambda^{(\text{rot})}$  can be defined in terms of  $Q^{(\text{rot})^*}$  as  $\lambda^{(\text{rot})} \equiv -Q^{(\text{rot})^*}/\Omega^{*2}$ , and it can be made dimensionless by defining  $\bar{\lambda}^{(\text{rot})} \equiv \bar{I}^2\bar{Q}$ . A quantity closely related with  $\lambda^{(\text{rot})}$  is the  $\ell = 2$  apsidal constant, defined as  $k_2^{(\text{rot})} \equiv (3/2)\lambda^{(\text{rot})}/R^5$ ; note that Berti et al. (2008) used a different definition. Following Colaiuda et al. (2008), we can also define the quadrupolar rotational ellipticity<sup>3</sup>  $e_Q^* \equiv -Q^{(\text{rot})^*}/I$ . Note that all of the

dimensionless quantities defined above are independent of the actual value of the rotation parameter  $\epsilon$ .

### 3.3 Tidally deformed neutron stars

We will also be interested in the tidal deformation of a *static* NS due the presence of an orbiting companion, e.g. in a binary system. The response to tidal deformations is encoded in the so-called  $\ell = 2$  tidal Love number  $\lambda^{(\text{tid})}$  (Hinderer 2008, 2009; Damour & Nagar 2009; Binnington & Poisson 2009), which is potentially measurable by advanced gravitational-wave interferometers. The tidal Love number can be put in a dimensionless form by defining  $\bar{\lambda}^{(\text{tid})} \equiv \lambda^{(\text{tid})}/M^5$ . We calculated the tidal Love number using the structure equations as presented by Postnikov et al. (2010), and validated our results by comparison against Yagi & Yunes (2013b).

### 3.4 Empirical relations for slowly rotating and tidally deformed neutron stars

We constructed NS models for all of the 14 EOS models listed in Table 1. We integrated the structure equations for central total energy densities within the range  $u_c \equiv \rho_c/\rho_0 \in [1.0, 2.0]$  in increments  $\Delta u_c = 0.1$ , for a total of 154 stellar models. We verified that the normalized binding energy  $M_b/M - 1$  (where  $M_b$  is the baryonic mass) is positive, so that all of these stellar configurations are bound.

Our results for the  $I$ -Love- $Q$  relations are shown in Fig. 3, which confirms the main findings of Yagi & Yunes (2013b): the universality holds within a few percent, except for very low-mass stars. This breakdown of the  $I$ -Love- $Q$  relations was already visible e.g. in Fig. 9 of Yagi & Yunes (2013b), but it is much more noticeable in the low-mass range explored in this work. Yagi et al. (2014b) suggested that the  $I$ -Love- $Q$  relations hold because of an approximate self-similarity in the star’s isodensity contours. This approximate symmetry only holds for compact stars, but it is broken in low-mass NSs, white dwarfs and ordinary stars. Indeed, the  $I$ -Love- $Q$  relations presented in Yagi et al. (2014b) were obtained by fitting data in the range  $\bar{Q} < 20$  and  $\bar{\lambda}^{(\text{tid})} < 2 \times 10^4$  (Yagi 2016).

In Fig. 4 we show that a universal “Love-Love” relation also holds between the tidal and rotational Love numbers. A well-known result in Newtonian gravity is that tidal and rotational Love numbers are the same (Mora & Will 2004). This equality no longer holds true for relativistic stars (Berti et al. 2008; Yagi & Yunes 2013b). Therefore we propose a different fit, namely:

$$\ln \bar{\lambda}^{(\text{rot})} = \sum_{j=0}^4 k_j \left( \ln \bar{\lambda}^{(\text{tid})} \right)^j, \quad (8)$$

where  $k_0 = 2.1089$ ,  $k_1 = 6.5084 \times 10^{-1}$ ,  $k_2 = 2.4688 \times 10^{-2}$ ,  $k_3 = -8.9891 \times 10^{-4}$  and  $k_4 = 1.3985 \times 10^{-5}$ . This fit uses

of the oblate rotating star, respectively. The surface ellipticity is related to the so-called “eccentricity”  $e \equiv [(r_e/r_p)^2 - 1]^{1/2}$  (see e.g. Berti et al. 2005) by  $e^2 = e_s^2 + 2e_s$ , and it describes the geometry of the star.

<sup>3</sup> This quantity is different from the surface ellipticity  $e_s \equiv r_e/r_p - 1$ , where  $r_e$  and  $r_p$  are the equatorial and polar radii

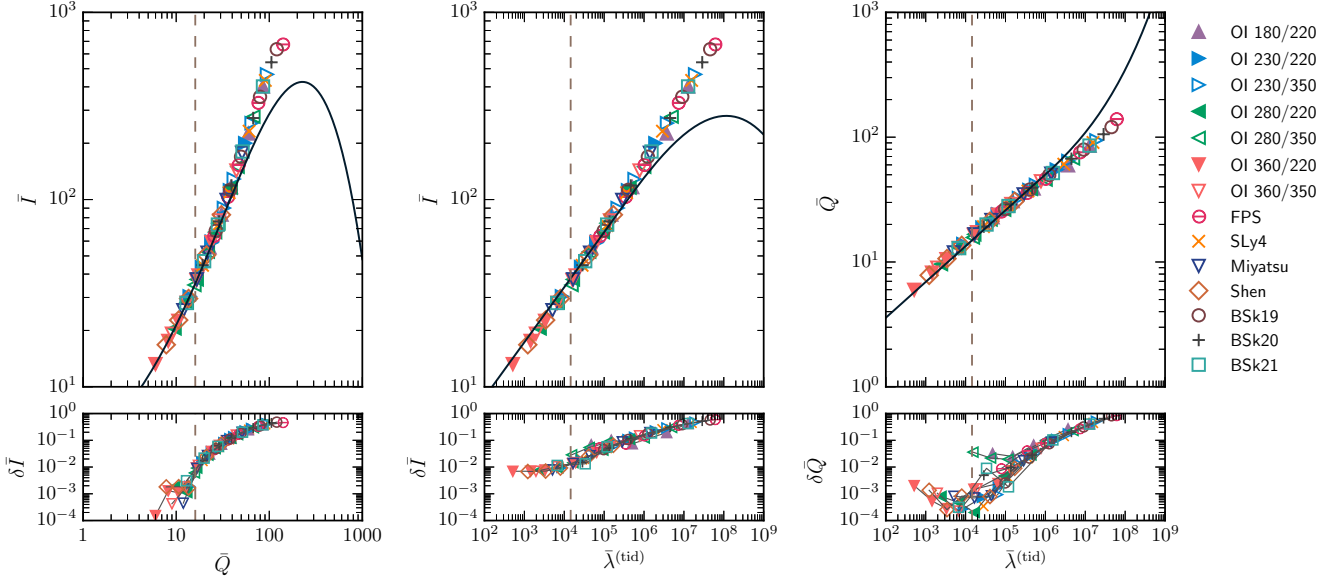


**Figure 3.** The EOS-independent  $I$ -Love- $Q$  relations (Yagi & Yunes 2013a,b) in the low-mass regime. The different panels show the  $I$ - $Q$  (left),  $I$ -Love (center) and Love- $Q$  (right) relations within the range of central energy densities considered here. For reference, the vertical dashed line corresponds to the values of  $\bar{Q}$  and  $\bar{\lambda}^{(\text{tid})}$  of a NS model using the Shen EOS with  $M/M_{\odot} = 0.89$ . The lower panels show that the fractional differences of the  $I$ -Love- $Q$  relations increases for very low mass (i.e., larger values of  $\bar{Q}$  and  $\bar{\lambda}^{(\text{tid})}$ ). Nevertheless, near and above the minimum mass value  $0.89 M_{\odot}$  the relations hold within an accuracy  $< 2\%$ . The explicit functional form of the  $I$ -Love- $Q$  relations can be found in Yagi & Yunes (2013b, Eq. (54) and Table 1).

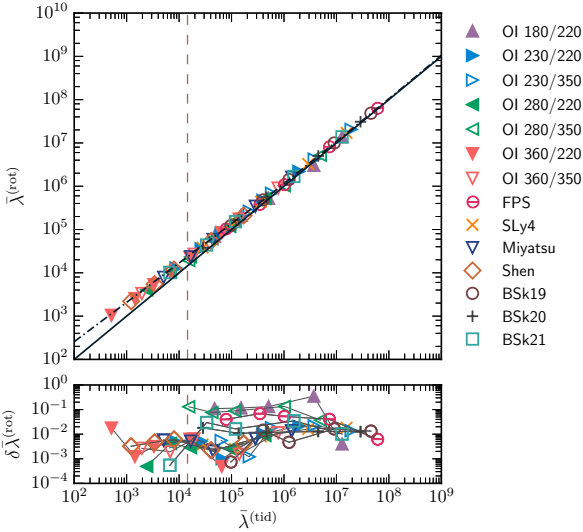


**Figure 4.** The EOS independent Love-Love relations in the low-mass regime. The Love-Love relation between  $\bar{\lambda}^{(\text{tid})}$  and  $\bar{\lambda}^{(\text{rot})}$  becomes an equality in the Newtonian – i.e., small- $M$  – limit (Mora & Will 2004), and deviates from unity for more relativistic stars (solid line). To make our fits of  $\bar{\lambda}^{(\text{tid})}$  and  $\bar{\lambda}^{(\text{rot})}$  with respect to  $\eta$  useful in combination with the Love-Love relation, we derived the improved fit of Eq. ((8)), corresponding to the dash-dotted line. This fit is accurate within  $< 1\%$  for  $M/M_{\odot} \geq 0.89$  (lower panel). The vertical dashed line corresponds to NS model with mass  $M/M_{\odot} = 0.89$  using the Shen EOS.

data in the central density range  $u_c \in [0.9, 2.0]$ , and it works accurately in the range of masses of our interest.

Using these numerical calculations we then fitted the various bulk properties of NSs as functions of  $\eta$  and of the central density. The quantities characterizing rotating stars – namely  $\bar{I}$ ,  $\bar{Q}$ , the  $\ell = 2$  rotational Love number  $\bar{\lambda}^{(\text{rot})} \equiv \bar{I}^2 \bar{Q}$ , the  $\ell = 2$  apsidal constant  $k_2^{(\text{rot})}$  and the quadrupolar ellipticity  $e_Q^*$  – are well fitted by functions of the form

$$\log_{10} y = c_0 \left( \frac{\eta}{100 \text{ MeV}} \right)^{c_1}. \quad (9)$$

Just as for the nonrotating bulk properties of NSs, the coefficients  $c_i$  depend on the ratio  $u_c \equiv \rho_c/\rho_0$ , which specifies the central density of the stellar model. Following Sotani et al. (2014), we fitted the  $c_i$ 's by quadratic polynomials of the form (6), so that each of our empirical formulas depends on six constant parameters  $c_{i,j}$ .

The quality of the fits is shown in the three panels of Fig. 5 for three representative bulk NS properties, namely the mass  $M$ , the dimensionless moment of inertia  $\bar{I}$  and the dimensionless quadrupole moment  $\bar{Q}$ . In summary: the non-rotating bulk properties of NSs can be expressed as functions of  $\eta$  of the form (5) combined with Eq. (6); the bulk properties of rotating and tidally deformed NSs can be fitted by functions of the form (9) combined with Eq. (6). The fitting coefficients are listed in Table 2, that collects the main results of our investigation.

The fits and their accuracy are also presented graphically in Figures 6–8. In the lower panel of each figure we plot the fractional differences  $\delta y$ . As in Fig. 2, the shaded area corresponds to the most plausible range of values for  $\eta$  as discussed in Sec. 2.2. These figures show that in general the

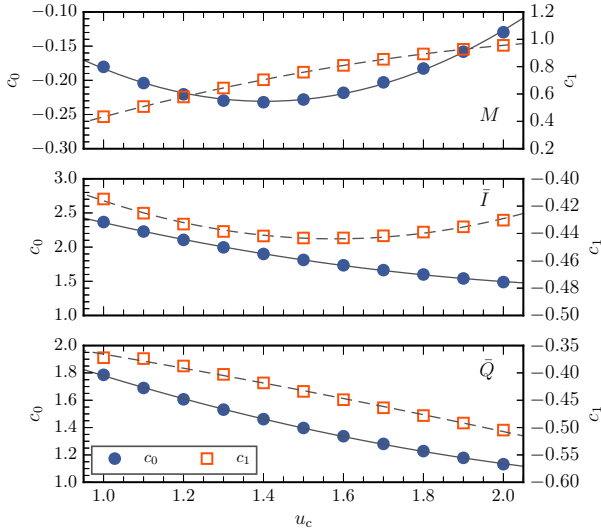


**Figure 5.** Illustration of the behavior of  $c_0$  (circles) and  $c_1$  (squares), appearing in the fitting expressions (5) and (9), as functions of  $u_c$ . The  $c_i$ 's are shown for three representative bulk properties of NSs: the mass  $M$  (top) fitted using Eqs. (5) and (6); the dimensionless moment of inertia  $\bar{I}$  (center) fitted using Eqs. (9) and (6); and the dimensionless quadrupole moment  $\bar{Q}$  (bottom) fitted using Eqs. (9) and (6).

fits work quite well in our fiducial range, i.e. for  $\eta > 67$  MeV, with larger errors for small  $\eta$ .

#### 4 CONCLUSIONS AND OUTLOOK

In this paper we have integrated the Hartle-Thorne equations for an extensive set of EOS models. We have computed the bulk properties of nonrotating (mass  $M$  and radius  $R$ , or equivalently mass  $M$  and surface redshift  $z$ ), rotating (moment of inertia  $I$ , quadrupole moment  $Q$ , quadrupole ellipticity  $e_Q$ , rotational Love number  $\lambda^{(\text{rot})}$ ,  $\ell = 2$  apsidal constant  $k_2^{(\text{rot})}$ ) and tidally deformed ( $\ell = 2$  tidal Love number  $\lambda^{(\text{tid})}$ ) low-mass NSs. All of these bulk NS properties can be fitted by relatively simple functions of the central density (more precisely, of  $u_c \equiv \rho_c/\rho_0$ ) and of the parameter  $\eta \equiv (K_0 L^2)^{1/3}$ , where  $K_0$  is the incompressibility of symmetric nuclear matter and  $L$  is the slope of the symmetry energy at saturation density. The coefficients of these fitting relations are summarized in Table 2.

The punchline of this work is that the measurement of *any two* of these bulk properties in low-mass NSs can be used – at least in principle – to infer the values of  $\rho_c$  and  $\eta$ , providing important information on the EOS. However there are some important practical caveats.

First and foremost – as shown in the lower panels of Figures 6–8 – the fitting relations are approximate, with relative errors that typically get larger for the lowest plausible values of  $\eta$ . Furthermore, as discussed in the literature, constraints on the bulk properties of NSs and on the EOS require Monte Carlo simulations or dedicated Bayesian studies which are beyond the scope of this paper (Steiner et al. 2010, 2013, 2015; Lattimer & Steiner 2014).

Even assuming accurate measurements of two of the

bulk properties of a given NS – to be concrete, say  $M$  and  $I$  – a conceptual limitation is that not all EOSs predict the existence of NSs with “realistic” masses (say,  $M > 0.89M_\odot$ ) in the range  $1 \leq u_c \leq 2$  where our fitting relations have been derived (cf. Fig. 1). This problem can in principle be circumvented, because the measurement of  $M$  and  $I$  can be used to infer *both*  $u_c$  and  $\eta$ , and thus to verify whether the NS really has central densities in the range of interest. However it is possible that systematic errors could spoil these consistency tests. For example one could imagine a situation where the “true” central density corresponds to (for example)  $u_c = 3$ , but since we are applying the fitting relations outside of their region of validity, we recover values of  $u_c \in [1, 2]$  and get a wrong estimate for  $\eta$  (Yagi 2016). These data analysis issues deserve further study.

The recent discovery of universal  $I$ -Love- $Q$  relations is also helpful. For example we can imagine measuring (say)  $M$ ,  $R$  and  $\bar{I}$  and getting information on the remaining bulk properties by exploiting the  $I$ -Love- $Q$  relations. A measurement of multiple parameters for the same astrophysical NS can be combined with our fitting formulas either to check the consistency of the inferred values of  $u_c$  and  $\eta$ , or to reduce statistical and/or systematic errors.

We conclude by speculating on some observational possibilities to implement this program.

Perhaps the most promising avenue in the near future is the measurement of mass and moment of inertia through relativistic spin-orbit coupling in systems such as the “double pulsar” PSR J0737-3039 (Burgay et al. 2003), especially considering that a 10% measurement of the moment of inertia *alone* can yield tight constraints on the pressure over a range of densities to within 50 – 60% (Steiner et al. 2015). This possibility was discussed by various authors (Damour & Schaefer 1988; Lattimer & Schutz 2005; Bejger et al. 2005). The experimental challenges associated with these measurements in the case of the double pulsar are reviewed (e.g.) in Section 6 of Kramer & Wex (2009).

In the near future it may also be possible to constrain  $\eta$  by gravitational-wave observations. Low-mass NSs are relatively promising gravitational-wave sources because they are more deformable and their crusts can support larger ellipticities, generating stronger gravitational-wave signals (Horowitz 2010; Johnson-McDaniel & Owen 2013; Johnson-McDaniel 2013, cf. also our Figs. 6 and 7). However the characteristic gravitational-wave amplitude depends on a (generally unknown) geometrical factor involving the orientation of the NS and the antenna pattern of the detectors (see e.g. Bonazzola & Gourgoulhon 1996; Dhurandhar et al. 2011). It has recently been proposed that gravitational-wave measurements of a *stochastic* gravitational-wave background from rotating NSs could be used to constrain the average NS ellipticity, and (if constraints on the masses can be obtained) these measurements could also constrain  $\eta$ . This possibility seems most promising for third-generation detectors such as the Einstein Telescope (Talukder et al. 2014).

Ono et al. (2015) proposed to estimate the mass of an isolated rapidly rotating NS by exploiting the mass-dependent logarithmic phase shift caused by the Shapiro time delay. According to their Monte Carlo simulations, the mass of a NS with spin frequency  $f = 500$  Hz and ellipticity  $10^{-6}$  at 1 kpc is typically measurable with an ac-

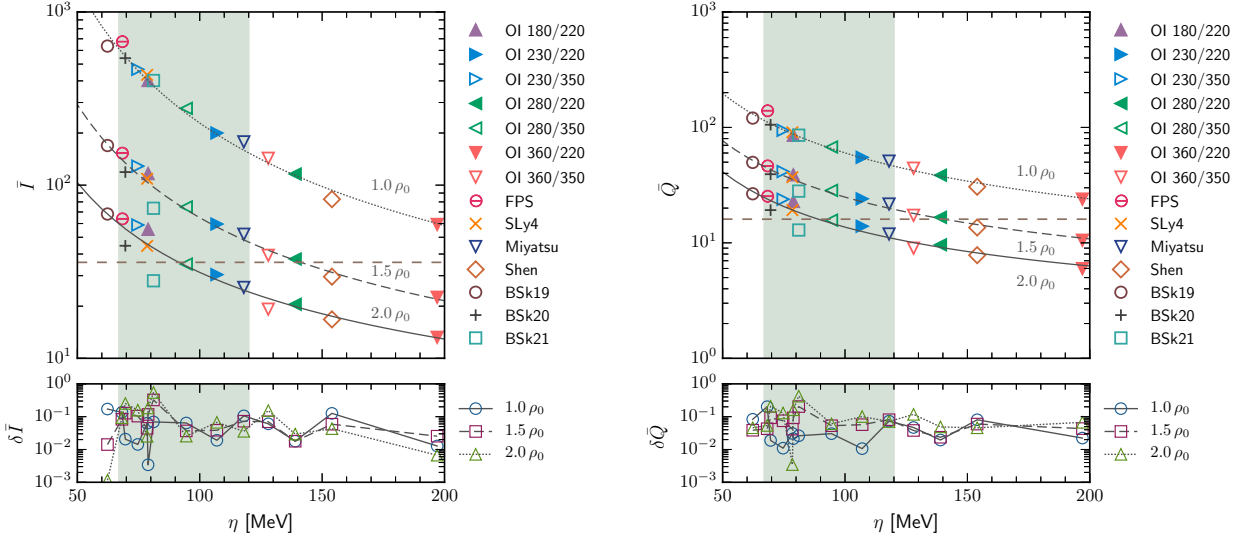


**Figure 6.** *Left:* fit of  $\bar{I} \equiv I/M^3$ . *Right:* Fit of the reduced quadrupole moment  $\bar{Q} \equiv Q^{(\text{rot})} / (M^3 \chi^2)$ . The horizontal dashed line in the left (right) panel marks the value of  $\bar{I}$  ( $\bar{Q}$ ) for a NS with  $M/M_\odot = 0.89$  and the Shen EOS.

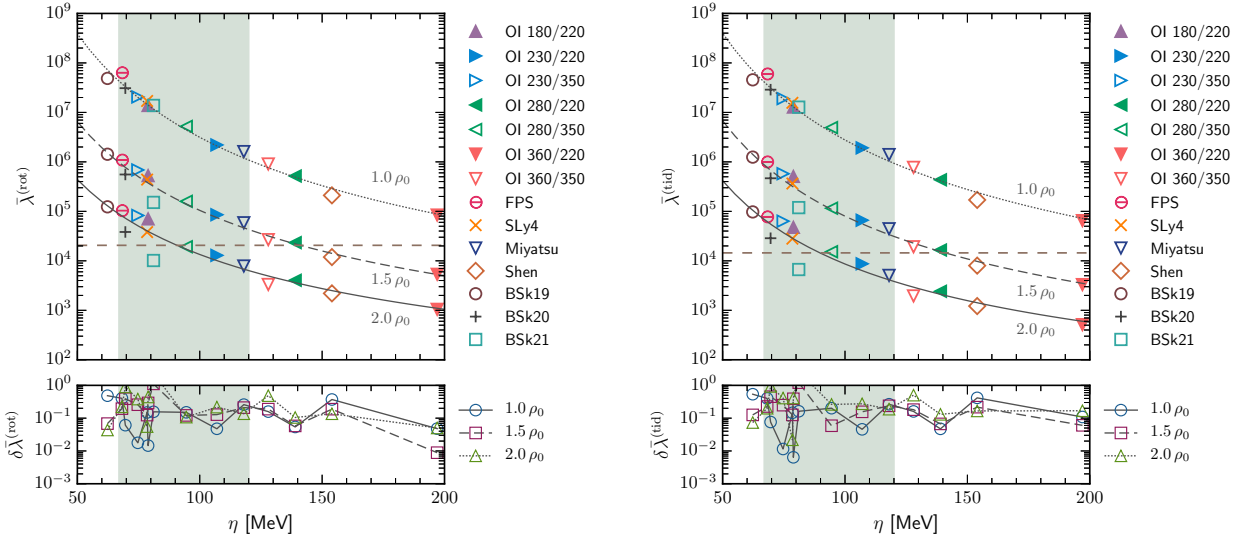


**Figure 7.** *Left:* Fit of the rotational Love number  $\bar{\lambda}^{(\text{rot})}$ . *Right:* Fit of the tidal Love number  $\bar{\lambda}_{\text{tid}}$ . The horizontal dashed line in the left (right) panel marks the value of  $\bar{\lambda}^{(\text{rot})}$  ( $\bar{\lambda}_{\text{tid}}$ ) for a NS with  $M/M_\odot = 0.89$  and the Shen EOS.

curacy of 20% using the Einstein Telescope. Higher-order terms in the Shapiro time delay will depend on the higher multipole moments  $I$  and  $Q$ , and they may allow us to measure these moments and constrain  $\eta$ . It may also be possible to combine the empirical relations of the present work with similar fitting relations that have been developed in the context of gravitational-wave asteroseismology (see e.g. Doneva & Kokkotas 2015).

Last but not least, as mentioned in the introduction, Advanced LIGO observations of binary systems involving NSs could yield measurements of masses and tidal Love numbers (Mora & Will 2004; Berti et al. 2008; Flanagan & Hinderer 2008; Read et al. 2009; Hinderer et al. 2010; Vines et al. 2011; Damour et al. 2012; Del Pozzo et al.

2013; Read et al. 2013; Lackey et al. 2014; Yagi & Yunes 2015; Dietrich et al. 2015). Recent studies pointed out that systematic errors on these measurements are large and that better waveform models are necessary (Favata 2014; Yagi & Yunes 2014; Chatziioannou et al. 2015b), but effective-one-body methods and numerical simulations are making remarkable progress in this direction (Bernuzzi et al. 2012, 2014, 2015a,b).

## ACKNOWLEDGEMENTS

We are indebted to Kent Yagi, Leo C. Stein and Nico Yunes for a very careful reading of an early draft of this paper, and

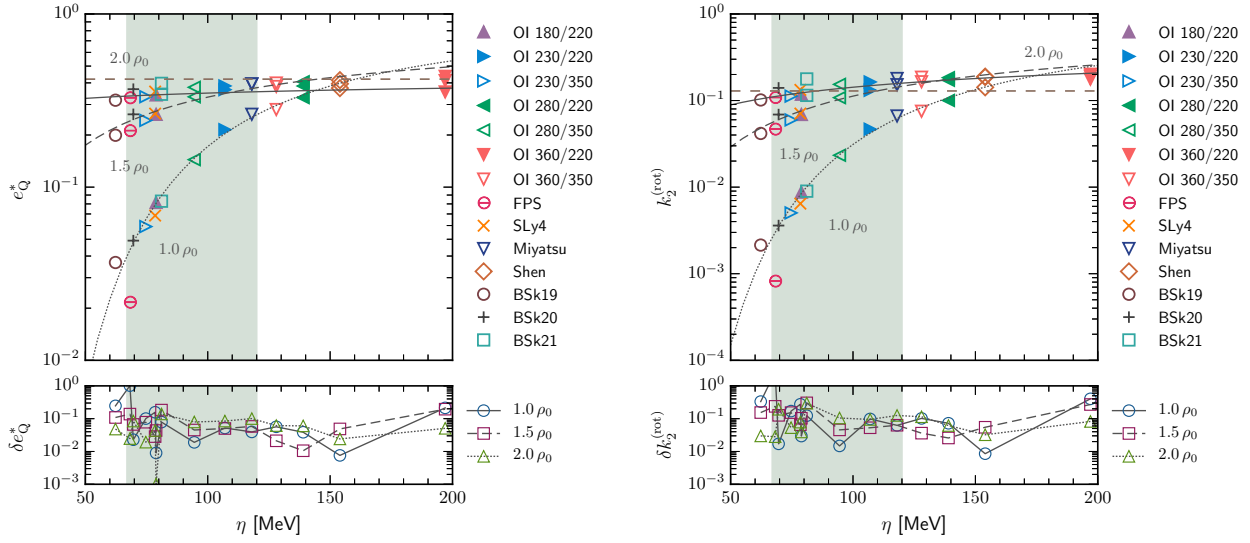


**Figure 8.** *Left:* Fit of the quadrupole ellipticity  $e_Q^*$ . *Right:* fit of the  $\ell = 2$  rotational apsidal constant  $k_2^{(\text{rot})}$ . Both quantities behave similarly, becoming nearly independent of  $\eta$  for  $\rho_c = 2.0\rho_0$ . For large value of  $\eta$ , we see that  $k_2^{(\text{rot})} \approx 0.7$  irrespective of the central density. The horizontal dashed line in the left (right) panel marks the value of  $e_Q^*$  ( $k_2^{(\text{rot})}$ ) for a NS with  $M/M_\odot = 0.89$  and the Shen EOS.

for valuable comments that significantly improved the paper. We thank Kei Iida, Kazuhiro Oyamatsu and Anthea F. Fantina for sharing some of the EOS data tables used in this work. We also thank Caio F.B. Macedo and Kent Yagi for validating some of our numerical results. E.B. was supported by NSF CAREER Grant No. PHY-1055103 and by FCT contract IF/00797/2014/CP1214/CT0012 under the IF2014 Programme. H.O.S. was supported by NSF CAREER Grant No. PHY-1055103 and by a Summer Research Assistantship Award from the University of Mississippi. E.B. and H.O.S. thank the Instituto Superior Técnico (Lisbon, Portugal), where this project started, for the hospitality. H.S. was supported by Grant-in-Aid for Young Scientists (B) through No. 26800133 provided by JSPS and by Grants-in-Aid for Scientific Research on Innovative Areas through No. 15H00843 provided by MEXT.

## REFERENCES

- Aasi J., et al., 2015, *Class. Quant. Grav.*, 32, 074001  
 Acernese F., et al., 2015, *Class. Quant. Grav.*, 32, 024001  
 Antoniadis J., Freire P. C., Wex N., Tauris T. M., Lynch R. S., et al., 2013, *Science*, 340, 6131  
 Bejger M., Bulik T., Haensel P., 2005, *Mon. Not. Roy. Astron. Soc.*, 364, 635  
 Belczynski K., Repetto S., Holz D., O’Shaughnessy R., Bulik T., Berti E., Fryer C., Dominik M., 2015, preprint ([arXiv:1510.04615](https://arxiv.org/abs/1510.04615))  
 Benhar O., Ferrari V., Gualtieri L., Marassi S., 2005, *Phys. Rev.*, D72, 044028  
 Bernuzzi S., Nagar A., Thierfelder M., Bruggmann B., 2012, *Phys. Rev.*, D86, 044030  
 Bernuzzi S., Nagar A., Balmelli S., Dietrich T., Ujevic M., 2014, *Phys. Rev. Lett.*, 112, 201101  
 Bernuzzi S., Nagar A., Dietrich T., Damour T., 2015a, *Phys. Rev. Lett.*, 114, 161103  
 Bernuzzi S., Dietrich T., Nagar A., 2015b, *Phys. Rev. Lett.*, 115, 091101  
 Berti E., Stergioulas N., 2004, *Mon. Not. Roy. Astron. Soc.*, 350, 1416  
 Berti E., White F., Maniopolou A., Bruni M., 2005, *MNRAS*, 358, 923  
 Berti E., Iyer S., Will C. M., 2008, *Phys. Rev. D*, 77, 024019  
 Berti E., et al., 2015, *Class. Quant. Grav.*, 32, 243001  
 Binnington T., Poisson E., 2009, *Phys. Rev.*, D80, 084018  
 Bonazzola S., Gourgoulhon E., 1996, *Astron. Astrophys.*, 312, 675  
 Brown D. A., Harry I., Lundgren A., Nitz A. H., 2012, *Phys. Rev.*, D86, 084017  
 Burgay M., et al., 2003, *Nature*, 426, 531  
 Chakrabarti S., Delsate T., Gürlbeck N., Steinhoff J., 2014, *Phys. Rev. Lett.*, 112, 201102  
 Chakrabarty D., 2008, *AIP Conf. Proc.*, 1068, 67  
 Chatziioannou K., Cornish N., Klein A., Yunes N., 2015a, *Astrophys. J.*, 798, L17  
 Chatziioannou K., Yagi K., Klein A., Cornish N., Yunes N., 2015b, *Phys. Rev.*, D92, 104008  
 Colaiuda A., Ferrari V., Gualtieri L., Pons J. A., 2008, *Mon. Not. Roy. Astron. Soc.*, 385, 2080  
 Cook G. B., Shapiro S. L., Teukolsky S. A., 1994, *Astrophys. J.*, 424, 823  
 Damour T., Nagar A., 2009, *Phys. Rev.*, D80, 084035  
 Damour T., Schaefer G., 1988, *Nuovo Cim.*, B101, 127  
 Damour T., Nagar A., Villain L., 2012, *Phys. Rev.*, D85, 123007  
 Del Pozzo W., Li T. G. F., Agathos M., Van Den Broeck C., Vitale S., 2013, *Phys. Rev. Lett.*, 111, 071101  
 Demorest P., Pennucci T., Ransom S., Roberts M., Hessels J., 2010, *Nature*, 467, 1081  
 Dhurandhar S., Tagoshi H., Okada Y., Kanda N., Takahashi H., 2011, *Phys. Rev.*, D84, 083007  
 Dietrich T., Moldenhauer N., Johnson-McDaniel N. K., Bernuzzi S., Markakis C. M., Brüggmann B., Tichy W., 2015, *Phys. Rev.*, D92, 124007  
 Dominik M., et al., 2015, *Astrophys. J.*, 806, 263  
 Doneva D. D., Kokkotas K. D., 2015, *Phys. Rev.*, D92, 124004  
 Doneva D. D., Yazadjiev S. S., Stergioulas N., Kokkotas K. D., 2013, *Astrophys. J.*, 781, L6  
 Douchin F., Haensel P., 2001, *Astron. Astrophys.*, 380, 151  
 Farr W. M., Sravan N., Cantrell A., Kreidberg L., Bailyn C. D.,

- Mandel I., Kalogera V., 2011, *Astrophys. J.*, 741, 103
- Favata M., 2014, *Phys. Rev. Lett.*, 112, 101101
- Feroci M., Herder J., Bozzo E., Barret D., Brandt S., et al., 2012, *Proc.SPIE*, 8443, 84432D
- Flanagan E. E., Hinderer T., 2008, *Phys. Rev.*, D77, 021502
- Friedman J. L., Stergioulas N., 2013, *Rotating Relativistic Stars*. Cambridge University Press, Cambridge
- Gandolfi S., Carlson J., Reddy S., 2012, *Phys. Rev.*, C85, 032801
- Gendreau K. C., Arzumanyan Z., Okajima T., 2012, in *Society of Photo-Optical Instrumentation Engineers (SPIE) Conference Series.*, doi:10.1117/12.926396
- Glampedakis K., Pappas G., Silva H. O., Berti E., 2015, *Phys. Rev.*, D92, 024056
- Goriely S., Chamel N., Pearson J. M., 2010, *Phys. Rev.*, C82, 035804
- Hartle J. B., 1967, *Astrophys. J.*, 150, 1005
- Hartle J. B., Thorne K. S., 1968, *ApJ*, 153, 807
- Hessels J. W. T., Ransom S. M., Stairs I. H., Freire P. C. C., Kaspi V. M., Camilo F., 2006, *Science*, 311, 1901
- Hinderer T., 2008, *ApJ*, 677, 1216
- Hinderer T., 2009, *ApJ*, 697, 964
- Hinderer T., Lackey B. D., Lang R. N., Read J. S., 2010, *Phys. Rev.*, D81, 123016
- Horowitz C. J., 2010, *Phys. Rev.*, D81, 103001
- Johnson-McDaniel N. K., 2013, *Phys. Rev.*, D88, 044016
- Johnson-McDaniel N. K., Owen B. J., 2013, *Phys. Rev.*, D88, 044004
- Khan E., Margueron J., 2013, *Phys. Rev.*, C88, 034319
- Kramer M., Wex N., 2009, *Class. Quant. Grav.*, 26, 073001
- Kreidberg L., Bailyn C. D., Farr W. M., Kalogera V., 2012, *Astrophys. J.*, 757, 36
- Lackey B. D., Kyutoku K., Shibata M., Brady P. R., Friedman J. L., 2014, *Phys. Rev.*, D89, 043009
- Lattimer J. M., 2012, *Ann. Rev. Nucl. Part. Sci.*, 62, 485
- Lattimer J., Prakash M., 2004, *Science*, 304, 536
- Lattimer J. M., Prakash M., 2007, *Phys. Rept.*, 442, 109
- Lattimer J. M., Prakash M., 2015, preprint (arXiv:1512.07820)
- Lattimer J. M., Schutz B. F., 2005, *Astrophys. J.*, 629, 979
- Lattimer J. M., Steiner A. W., 2014, *Eur. Phys. J.*, A50, 40
- Lau H. K., Leung P. T., Lin L. M., 2010, *Astrophys. J.*, 714, 1234
- Li B.-A., Han X., 2013, *Phys. Lett.*, B727, 276
- Li B.-A., Ramos A., Verde G., Vidana I., 2014, *Eur. Phys. J.*, A50, 9
- Littenberg T. B., Farr B., Coughlin S., Kalogera V., Holz D. E., 2015, *Astrophys. J.*, 807, L24
- Lo K.-W., Lin L.-M., 2011, *Astrophys. J.*, 728, 12
- Lorenz C. P., Ravenhall D. G., Pethick C. J., 1993, *Phys. Rev. Lett.*, 70, 379
- Lorimer D. R., 2001, *Living Rev. Rel.*, 4, 5
- Mandel I., O'Shaughnessy R., 2010, *Class. Quant. Grav.*, 27, 114007
- Mandel I., Haster C.-J., Dominik M., Belczynski K., 2015, *Mon. Not. Roy. Astron. Soc.*, 450, L85
- Martinez J. G., et al., 2015, *Astrophys. J.*, 812, 143
- Miyatsu T., Yamamuro S., Nakazato K., 2013, *Astrophys. J.*, 777, 4
- Mora T., Will C. M., 2004, *Phys. Rev.*, D69, 104021
- Newton W. G., Hooker J., Gearheart M., Murphy K., Wen D.-H., Fattoyev F. J., Li B.-A., 2014, *European Physical Journal A*, 50, 41
- Ono K., Eda K., Itoh Y., 2015, *Phys. Rev.*, D91, 084032
- Oyamatsu K., Iida K., 2003, *Prog. Theor. Phys.*, 109, 631
- Ozel F., Psaltis D., Narayan R., McClintock J. E., 2010, *Astrophys. J.*, 725, 1918
- Pappas G., Apostolatos T. A., 2014, *Phys. Rev. Lett.*, 112, 121101
- Pearson J. M., Goriely S., Chamel N., 2011, *Phys. Rev. C*, 83, 065810
- Pearson J. M., Chamel N., Goriely S., Ducoin C., 2012, *Phys. Rev. C*, 85, 065803
- Popov S. B., Blaschke D., Grigorian H., Prokhorov M. E., 2007, *Astrophys. Space Sci.*, 308, 381
- Postnikov S., Prakash M., Lattimer J. M., 2010, *Phys. Rev.*, D82, 024016
- Potekhin A. Y., Fantina A. F., Chamel N., Pearson J. M., Goriely S., 2013, *Astron. Astrophys.*, 560, A48
- Psaltis D., 2008, *Living Rev. Rel.*, 11, 9
- Read J. S., Markakis C., Shibata M., Uryu K., Creighton J. D. E., Friedman J. L., 2009, *Phys. Rev.*, D79, 124033
- Read J. S., et al., 2013, *Phys. Rev.*, D88, 044042
- Sathyaprakash B., et al., 2012, *Class. Quant. Grav.*, 29, 124013
- Shapiro S., Teukolsky S., 1983, *Black holes, white dwarfs, and neutron stars: The physics of compact objects*. Wiley
- Shen H., Toki H., Oyamatsu K., Sumiyoshi K., 1998, *Nucl. Phys.*, A637, 435
- Somiya K., 2012, *Class. Quant. Grav.*, 29, 124007
- Sotani H., Nakazato K., Iida K., Oyamatsu K., 2013, *Mon. Not. Roy. Astron. Soc.*, 434, 2060
- Sotani H., Iida K., Oyamatsu K., Ohnishi A., 2014, *PTEP*, 2014, 051E01
- Sotani H., Iida K., Oyamatsu K., 2015, *Phys. Rev.*, C91, 015805
- Sotani H., Iida K., Oyamatsu K., 2016, *New Astron.*, 43, 80
- Steiner A. W., Prakash M., Lattimer J. M., Ellis P. J., 2005, *Phys. Rept.*, 411, 325
- Steiner A. W., Lattimer J. M., Brown E. F., 2010, *Astrophys. J.*, 722, 33
- Steiner A. W., Lattimer J. M., Brown E. F., 2013, *Astrophys. J.*, 765, L5
- Steiner A. W., Gandolfi S., Fattoyev F. J., Newton W. G., 2015, *Phys. Rev.*, C91, 015804
- Stergioulas N., 2003, *Living Rev. Relativ.*, 6, 3
- Stevenson S., Ohme F., Fairhurst S., 2015, *Astrophys. J.*, 810, 58
- Strobel K., Schaab C., Weigel M. K., 1999, *Astron. Astrophys.*, 350, 497
- Suleimanov V., Poutanen J., Revnivtsev M., Werner K., 2011, *Astrophys. J.*, 742, 122
- Sumiyoshi K., Ibáñez J. M., Romero J. V., 1999, *A&AS*, 134, 39
- Takahashi T., et al., 2012, *Proc. SPIE Int. Soc. Opt. Eng.*, 8443, 1Z
- Talukder D., Thrane E., Bose S., Regimbau T., 2014, *Phys. Rev.*, D89, 123008
- Tauris T. M., Langer N., Podsiadlowski P., 2015, *Mon. Not. Roy. Astron. Soc.*, 451, 2123
- Tsang M. B., Zhang Y., Danielewicz P., Famiano M., Li Z., Lynch W. G., Steiner A. W., 2009, *Phys. Rev. Lett.*, 102, 122701
- Tsang M. B., et al., 2012, *Phys. Rev.*, C86, 015803
- Vines J., Flanagan E. E., Hinderer T., 2011, *Phys. Rev.*, D83, 084051
- Watts A., et al., 2015, *PoS, AASKA14*, 043
- Yagi K., 2016, private communication
- Yagi K., Yunes N., 2013a, *Science*, 341, 365
- Yagi K., Yunes N., 2013b, *Phys. Rev.*, D88, 023009
- Yagi K., Yunes N., 2014, *Phys. Rev. D*, 89, 021303
- Yagi K., Yunes N., 2015, preprint (arXiv:1512.02639)
- Yagi K., Kyutoku K., Pappas G., Yunes N., Apostolatos T. A., 2014a, *Phys. Rev.*, D89, 124013
- Yagi K., Stein L. C., Pappas G., Yunes N., Apostolatos T. A., 2014b, *Phys. Rev.*, D90, 063010
- Yasuda J., et al., 2013, *PTEP*, 2013, 063D02

This paper has been typeset from a  $\text{\TeX}/\text{\LaTeX}$  file prepared by the author.